

## Research Article

# One-Pot Synthesis of Photoluminescent Self-Assembled Carbon Dot Monolayer Films

Hongchong Guo,<sup>1</sup> Wei Li,<sup>1</sup> Gang Sun,<sup>2</sup> and Bo You <sup>1</sup>

<sup>1</sup>Department of Materials Science and the Advanced Coatings Research Center of the China Educational Ministry, Fudan University, Shanghai 200433, China

<sup>2</sup>Department of Aeronautics and Astronautics, Fudan University, Shanghai 200433, China

Correspondence should be addressed to Bo You; [youbu@fudan.edu.cn](mailto:youbu@fudan.edu.cn)

Received 12 December 2018; Revised 25 February 2019; Accepted 26 February 2019; Published 4 April 2019

Guest Editor: Nour F. Attia

Copyright © 2019 Hongchong Guo et al. This is an open access article distributed under the Creative Commons Attribution License, which permits unrestricted use, distribution, and reproduction in any medium, provided the original work is properly cited.

We propose a facile and simple synthesis of photoluminescent (PL) carbon dot self-assembled monolayer films (CD-SAMFs) at oil-water interfaces. By using styrene both as the carbon source and the oil phase medium, we got our amazing CD-SAMFs under the copper acetate and hydrogen peroxide ( $\text{Cu}(\text{Ac})_2\text{-H}_2\text{O}_2$ ) catalytic-oxidation system. Without any surface modification, the spontaneously formed CD-SAMFs exhibit ultrathin thickness ( $<10\text{ nm}$ ), bright luminescence, high transparency, and hydrophobicity, which have the potential as a new alternative to be used on multifunctional coating films, anticounterfeiting, displays, sensors, and optical devices.

## 1. Introduction

The advent of two-dimensional (2D) materials opens up new opportunities and challenges [1]. Most notably, self-assembled monolayers (SAMs) have served as an excellent candidate for the fabrication of technologically important ultrathin film materials for sensors, optical devices, and magnetic storage media [2–7]. In particular, semiconductor quantum dot (QD: CdTe or CdSe/ZnS) SAMs have advantageous features in the field of luminescent materials [8–10]. However, compared to these traditional quantum dots, carbon quantum dots (CDs), as a new class of nanomaterial, possessed captivating properties such as excellent photostability, low toxicity, low cost, and easy synthesis [11, 12]. Recently, the self-assembly monolayers of the carbon nanoparticles on metal surfaces hold great potential for novel electronic and optoelectronic properties [13–16]. However, there is rarely any report about the methods of CD self-assembled films.

Here, we developed a simple and one-pot synthesis of carbon dot self-assembled monolayer films (CD-SAMFs). By using styrene both as the reactant (carbon source) and

oil phase medium, the CD-SAMFs formed at the oil-water interfaces through copper acetate and hydrogen peroxide ( $\text{Cu}(\text{Ac})_2\text{-H}_2\text{O}_2$ ) catalytic oxidation. Without modified agents or harsh conditions (such as Chemical Vapor Deposition (CVD), electrophoresis deposition, and layer-by-layer (LBL) self-assembly) [13–18], the as-produced hydroxyl-enriched CDs can be spontaneously self-assembled into the carbon dot monolayer films via hydrogen bond interactions. The ultrathin CD-SAMFs ( $<10\text{ nm}$ ) possessed brightly luminescent, highly transparent, and hydrophobic properties. Besides, this method can also help other benzene series including benzene, benzyl alcohol, and xylene be converted to CDs under the same conditions, which is an environmentally friendly way to reuse these volatile organic compound (VOC) wastes and is very promising for industrial application.

The one-pot synthesis of the CD-SAMFs is as follows: deionized water,  $\text{Cu}(\text{Ac})_2$ ,  $\text{H}_2\text{O}_2$ , and styrene were added to a 100 mL conical flask with stopper under stirring at 60 degrees Celsius. The system was sealed at the designated temperature for 12 hours. As shown in Figure 1(a), when the  $\text{H}_2\text{O}_2$  was added into the blue  $\text{Cu}(\text{Ac})_2$  solution, the color

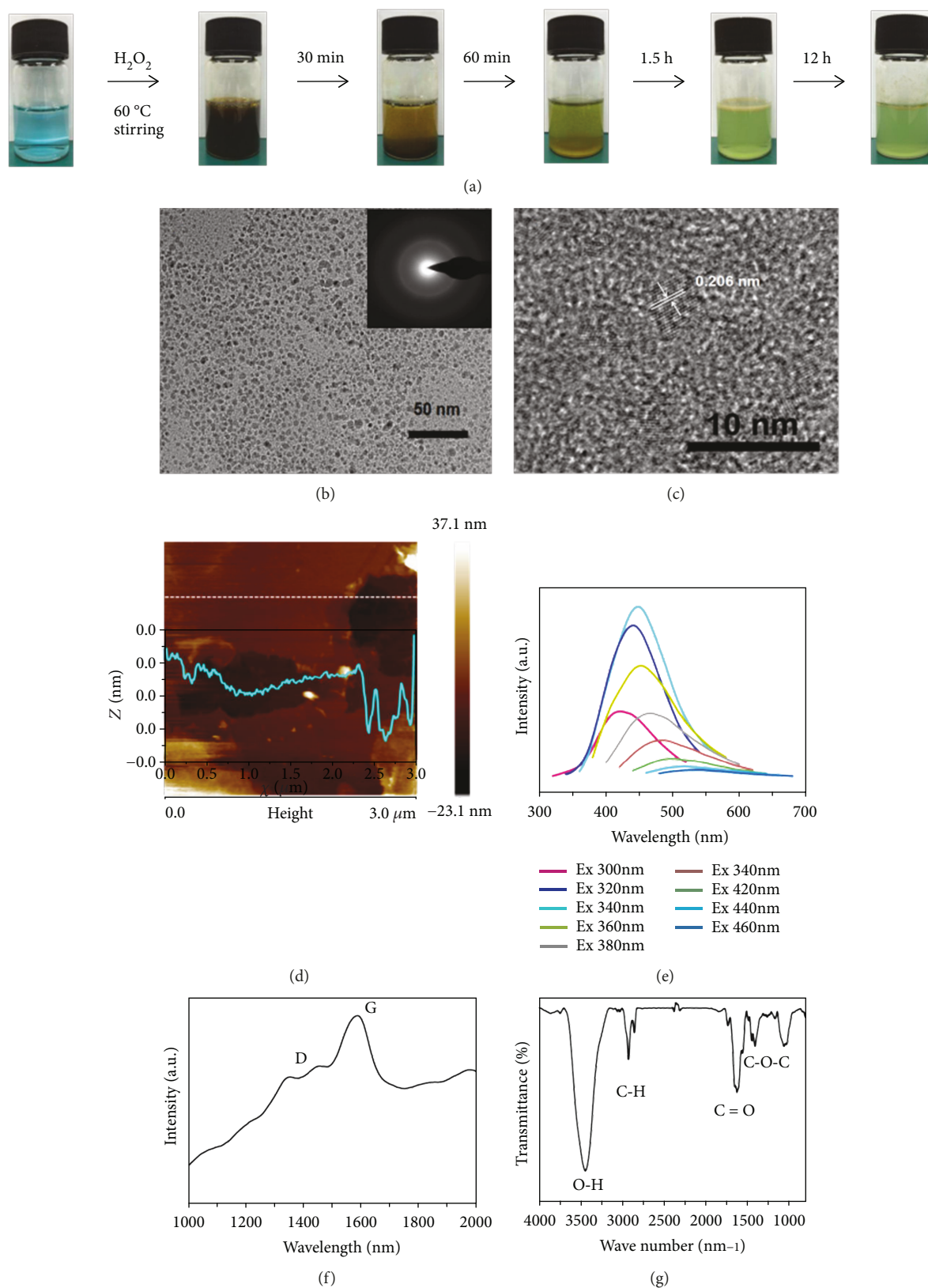


FIGURE 1: Preparation and structural characterization of CD-SAMFs: (a) Synthetic procedure; (b, c) HRTEM images and SAED; (d) AFM images, inset: height profile of cross-sections of the monolayers, Z: height (nm); s: distance ( $\mu m$ ); (e) PL emission spectra based on different excitation wavelength; (f) Raman spectrum; (g) FTIR spectrum.

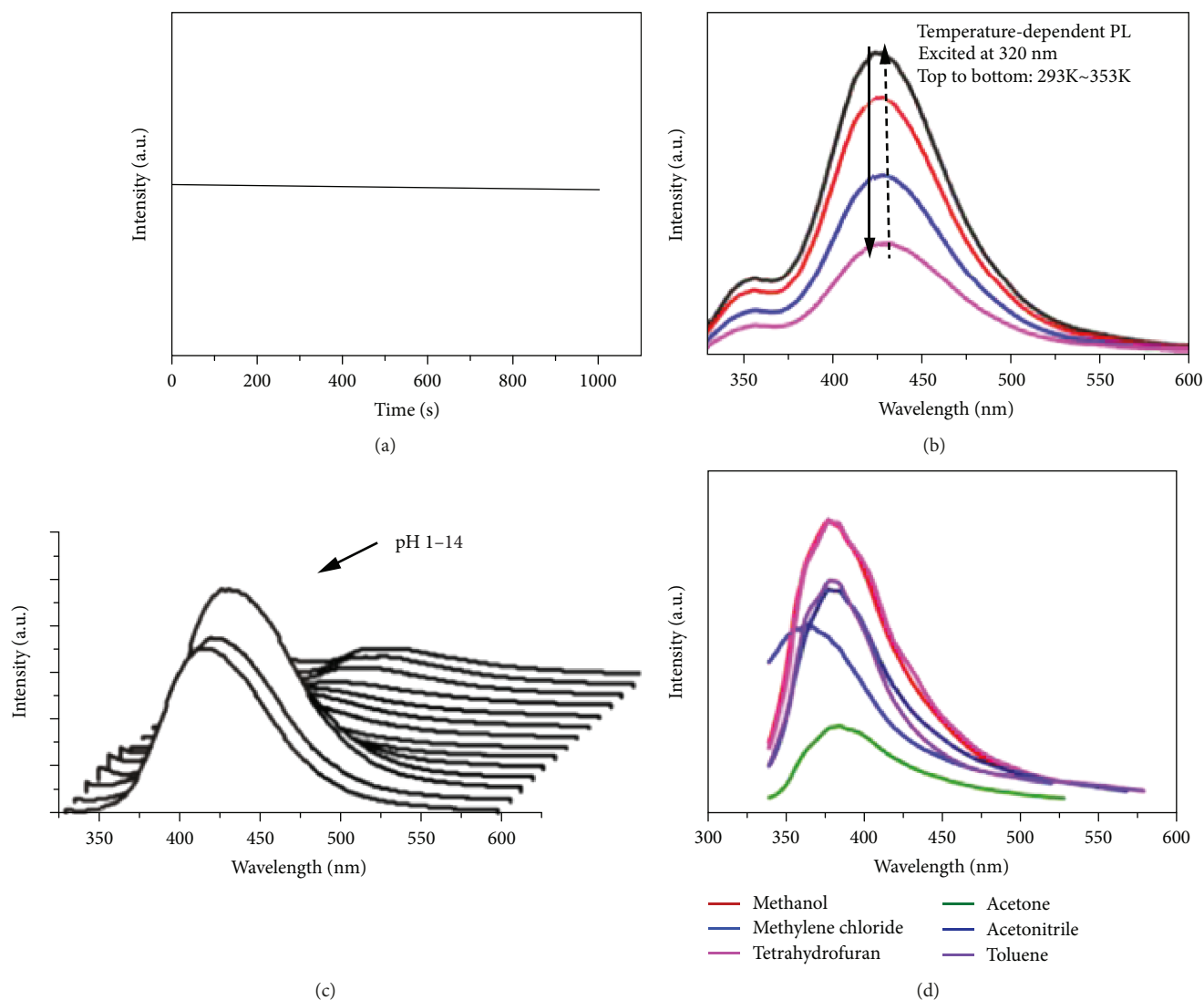


FIGURE 2: PL properties of CD-SAMFs: (a) time-based PL spectrum; (b) temperature-dependent PL spectra from 293 to 353 K at 320 nm excitation; (c) pH-dependent PL spectra; (d) PL emission spectra of CD-SAMFs dispersed in different polar solvents.

of the solution rapidly turned from blue to red brown, then became yellow. About one and a half hour later, the solution turned green eventually. Some cream-colored products were suspended on the surface of the solution. It is possible that a lot of copper intermediates of different oxidation state were produced; meanwhile, a large quantity of CDs was produced, which then self-assembled to the carbon dot nanofilms at the oil-water interfaces between the styrene oil phase and the solution. As shown in Figures 1(b) and 1(c), the high-resolution transmission electron microscopy (HRTEM) images revealed that the CDs were self-assembled to the ultrathin carbon dot nanofilms. The CDs were well dispersed with a Gaussian size distribution and an average size of  $4.75 \pm 0.58$  nm (Figure S1), which presented good uniformity. HRTEM images confirmed the CDs' crystalline nature and revealed a lattice spacing of  $0.203 \pm 0.003$  nm (Figure 1(c)), which corresponds to the (111) diffraction plane of the diamond structure [19]. The atomic force microscope (AFM) images showed that the

ultrathin carbon dot nanofilm was about  $<10$  nm high (Figure 1(d) inset), which was consistent with the lateral sizes of the CDs and further demonstrated that the film was a monolayer. The resultant fluorescence spectra obviously showed that CD-SAMFs possessed a multiemission nature depending on the excitation wavelength, which might rely not only on the energy gap governed by the surface oxidation states and the size of the CDs [20] but also on the different emissive sites on each carbon dot [21] (Figure 1(e) and Figure S2 for other benzene series VOCs). As the excitation wavelength changed from 300 nm to 500 nm, the emission exhibited an obvious red shift from 400 nm to 540 nm correspondingly, which displayed an emission maximum at 450 nm under excitation at wavelength 340 nm. The UV-Vis spectra of benzene series-CDs presented a broad absorption band (200-600 nm) as previously reported [21]. A clear shoulder absorption peak of styrene CDs at 230 nm was attributed to the  $\pi$ -electron system, suggesting the existence of the  $sp^2$  aromatic

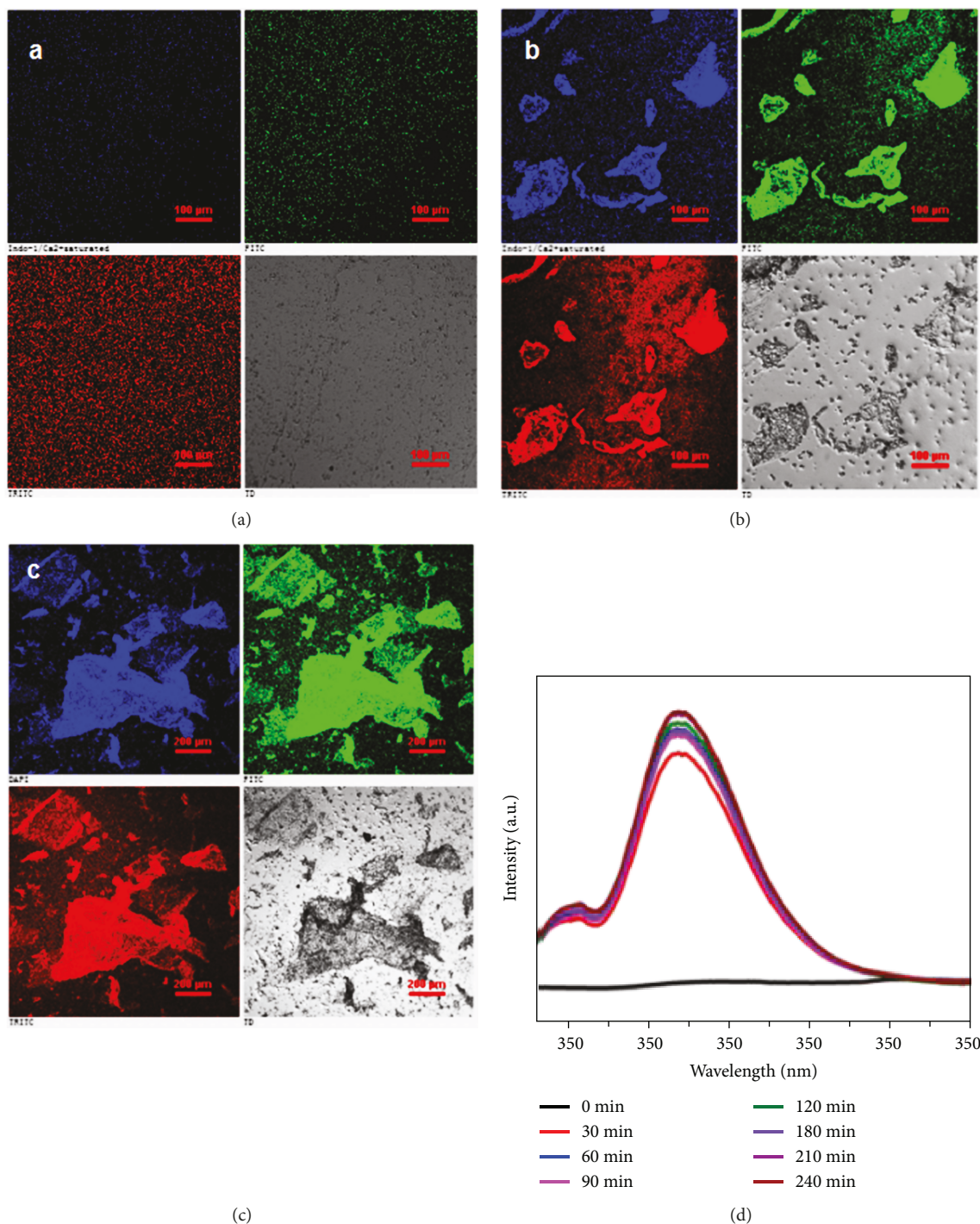


FIGURE 3: Fluorescent images of CD-SAMFs at different reaction times: (a) 10 min, (b) 60 min, (c) 12 h, and (d) PL emission spectra of CD-SAMFs (Ex = 340 nm). Scale: (a, b) 100  $\mu\text{m}$ , (c) 200  $\mu\text{m}$ .

structure units [22], which might originate from the impurities of the styrene (Figure S2). As shown in Figure 1(f), a strong Raman signature from the G band assigned to  $\text{sp}^2$  carbons appeared at the energy peak of  $1590\text{ cm}^{-1}$ . Its intensity was much higher than the  $\text{sp}^3$  Raman peak (D band at  $1338\text{ cm}^{-1}$ ), which indicated the large degree of graphitization of CDs (Figure S3) [23]. FTIR results further indicated that all the CDs are

abundant oxygen-containing functional groups (carbonyl and hydroxyl group) (Figure 1(g) and Figure S4).

The CD-SAMFs possessed high photostability at 1000s (Figure 2(a)) and reversible thermosensitivity with the temperature varying from 293 K to 393 K (Figure 2(b)). Another interesting phenomenon was the pH-dependent behavior as the PL intensities increased in solutions with high pH values, while they almost kept stable when the pH was changed from

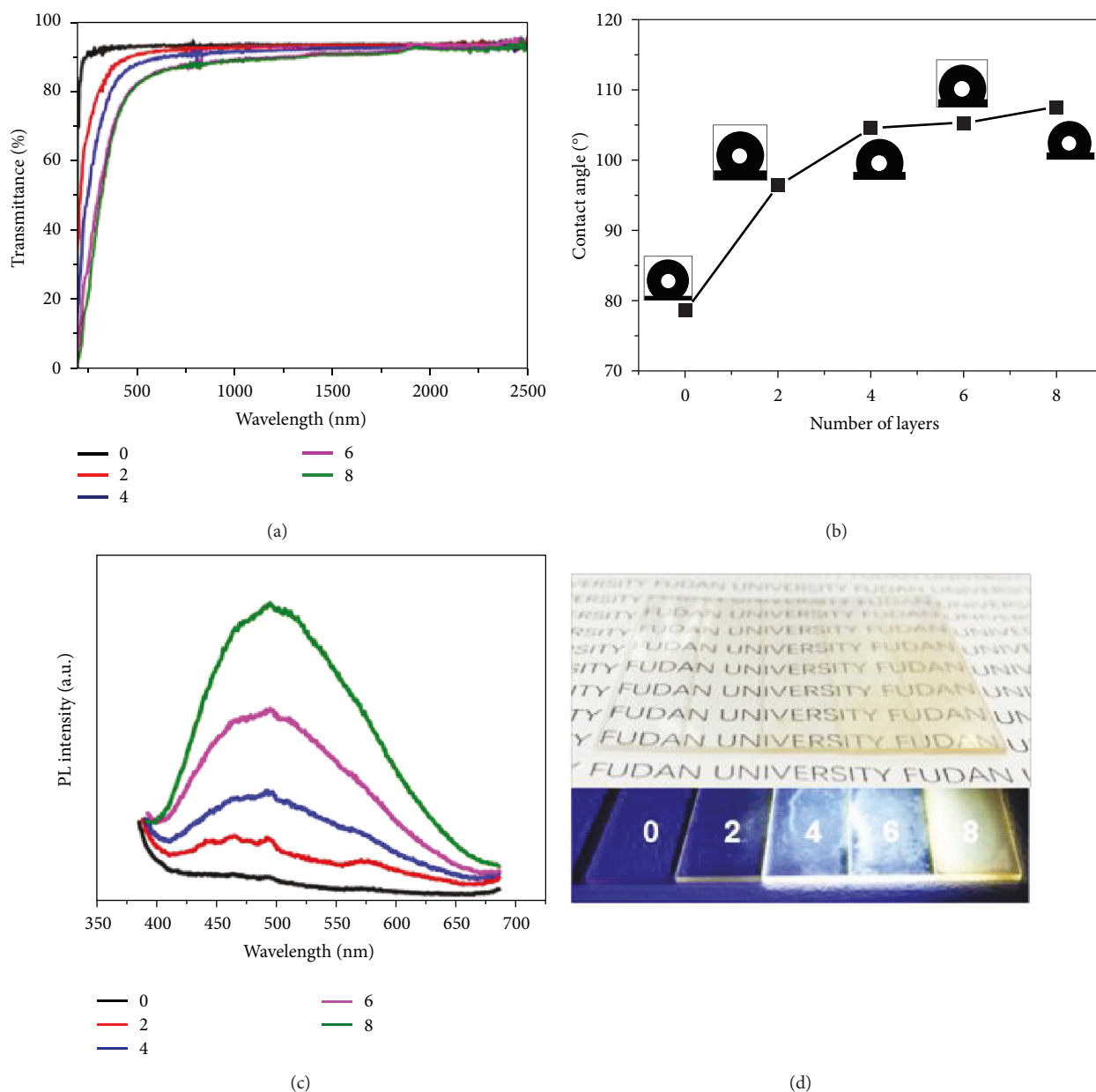
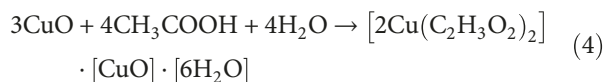
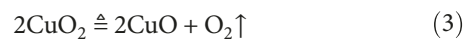
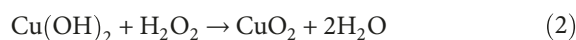
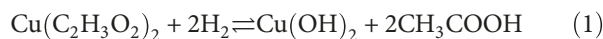


FIGURE 4: Optical transmittance and hydrophobicity test. (a) Transmittance of the control (quartz glass) and multilayer CD-SAMFs on the quartz glass. (b) Water contact angle of the control and CD-SAMFs on the quartz glass. (c) PL emission spectra of CD-SAMFs (Ex = 365 nm). (d) Photographs of these CD-SAMFs under visible light (top) and UV irradiation (365 nm) (down).

1 to 11 (Figure 2(c)). Without any surface passivation, the acquired CDs exhibited fluorescent properties and well dispersion in organic solvents (such as methanol, methylene chloride, tetrahydrofuran, acetone, acetonitrile, and toluene) (Figure 2(d)).

The formation mechanism of the CD-SAMFs in the  $\text{Cu}(\text{Ac})_2\text{-H}_2\text{O}_2$  system is through the catalytic-oxidation reaction at the oil-water interfaces. Different from the self-assembled nanospheres via CDs in a copper sulfate and hydrogen peroxide ( $\text{CuSO}_4\text{-H}_2\text{O}_2$ ) catalytic-oxidation system as our previous work presented [24], copper acetate is a weak acid and weak base salt (pH 4.8), so the divalent copper ion and the acetate radical were hydrolyzed to form

copper hydroxide and acetic acid firstly (step 1). When  $\text{H}_2\text{O}_2$  was added to the solution, the whole possible reaction could be proposed as follows:



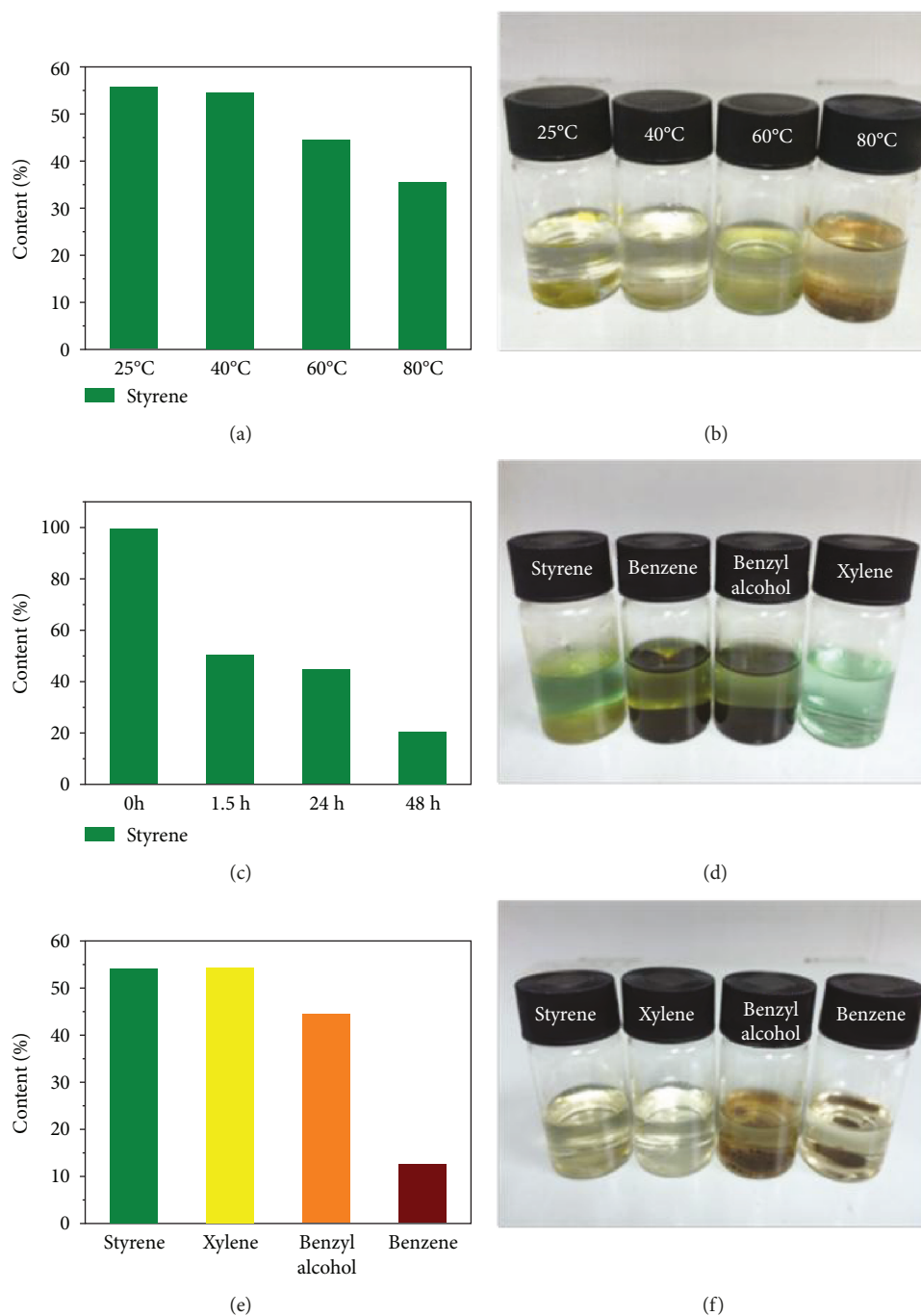


FIGURE 5: Degradation of benzene series VOCs by GC-MS test. (a, b) The content and the photograph of the styrene after reaction at different temperatures (24 h). (c) The content of styrene after reaction at different reaction times at 60°C. (d–f) The raw solution, the content, and the butyl acetate extract of benzene series VOCs after reaction (24 h) at 25°C, respectively.

Then, copper hydroxide reacted with hydrogen peroxide to form copper peroxide (step 2). With the heating of the reaction process, the brown copper peroxides decomposed, accompanied by a large amount of heat and  $O_2$  (step 3). In the weak acid solution, the resulting copper oxide reacted with acetic acid to form copper acetate. Meanwhile, a large amount of oxygen produced in the whole process acted as the oxidant for the oxidation of the styrene, resulting in the formation of carbon clusters  $C_2$ ,  $C_3$ ,  $C_2H_2$ , other small

molecules, and hydrogen ions, which finally crystallized into CDs in the solution rather than further be oxidized into  $CO_x$  owing to the weak oxidation of the  $O_2$ . In addition, the brownish copper peroxide gradually disappeared after the reaction, and the solution became green instead of the original blue, which means the basic copper acetate salts ( $[2Cu(C_2H_3O_2)_2] \cdot [CuO] \cdot [6H_2O]$ ) were formed (step 4).

During the reaction process, more and more CDs are produced. As the unreacted reactant styrene and the solution

formed two phases, self-assembled CD monolayer films appeared at the oil-water interfaces. As is shown in Figure 3, the fragments of the CD-SAMFs were first formed after 60 minutes as observed by the fluorescence microscope (Figures 3(a) and 3(b)). Then, about 12 hours later, these small fragments self-assembled into large-scale monolayer films (Figure 3(c)). In general, the fluorescence of CDs is always strongly quenched when large quantities of CDs are deposited on glass, metal, silicon, or plastic substrates owing to the formation of aggregates. However, the bright emission of the CD-SAMFs may have resulted from the self-assembly of the CDs via hydrogen bonding interaction, preventing aggregation-induced quenching [25, 26]. The fluorescence spectra also recorded this phenomenon exactly. About 60 minutes later, the fluorescence emission intensity dramatically rose to almost the maximum and then increased gently within four hours (Figure 3(d)).

Moreover, the CD-SAMFs possessed high transparency and hydrophobicity. As is shown in Figure 4(a), the transmittance of these CD-SAMFs decreased slowly with the multilayer number varying from 2 to 8. And the transmittance of different numbers of multilayers was all above 80% at the UV-Vis and near infrared band ( $>480$  nm), which indicated that the CD-SAMFs can become favorable candidates for optics applications [27]. In addition, it was found that the water contact angle (WCA) with increasing multilayer CD-SAMFs was increased from  $98^\circ$  to  $108^\circ$  ( $>90^\circ$ ), which means the ultrathin CD nanofilms possessed a hydrophobic surface (Figure 4(b)). Like the diamond-like carbon (DLC) films, the good transparency and hydrophobicity of the CD-SAMFs is possibly attributed to the diamond-like structures of the CDs [28]. Although small vacancies between adjacent CDs and the aggregation still existed, the WCA of the multilayer CD-SAMFs increased with the increasing number of the multilayers. It is possible that the multilayer CD-SAMFs make up for those minor defects in the CD monolayer [10]. Moreover, the PL emission spectra of CD-SAMFs showed that the PL intensities of the fluorescence bands at about 500 nm increased gradually with the increasing number of multilayers  $n$  and the CD-SAMFs emitted green light under UV irradiation (Figures 4(c) and 4(d)). Additionally, it was noteworthy that there was no significant shift or broadening of the emission band for different values of  $n$ , which demonstrated that there were no obvious changes in intermolecular interactions or of the nature of CDs in the whole assembly process as per previous reports [10].

What is more, this method may also provide a new approach to highly effectively degrade benzene series VOC waste water. During the reaction, the higher the temperature, the more CDs are produced. As is shown in Figure 5, when the temperature was increasing from  $25^\circ\text{C}$  to  $80^\circ\text{C}$ , the styrene was greatly reduced from 56% to 36% after the reaction for 24 h (Figures 5(a) and 5(b)). Keeping the reaction temperature at  $60^\circ\text{C}$ , Figure 5(c) indicates that the content of styrene decreased from 51% to 21% along the reaction from 1.5 h to 48 h. Other benzene series VOCs could also be converted to CDs (Table S1), and the content of the xylene and benzyl alcohol was about 55% and 45%, respectively, but the content of benzene was greatly decreased to 12.8% after

24 h reaction at  $25^\circ\text{C}$ , which was possibly attributed to the stronger reducibility than that of other benzene series (Figures 5(d)–5(f)).

## 2. Conclusions

In summary, we have developed a facile and one-pot synthesis of PL CD-SAMFs at the oil-water interfaces by  $\text{Cu}(\text{Ac})_2\text{-H}_2\text{O}_2$  catalytic-oxidation reaction. Different from the semiconductor QDs, the hydroxyl-enriched CDs can be spontaneously self-assembled to the carbon dot monolayer films via hydrogen bond interactions at the oil-water interfaces without any surface modification. The as-produced CD-SAMFs by the diamond-like CDs possessed ultrathin thickness ( $<10$  nm), which was comparable to the diamond-like carbon (DLC) films. With increase of the multilayer number, the PL intensities and the hydrophobicity were also enhanced. Moreover, their superior performances with high transparency and hydrophobicity showed potential application for multifunctional coating films, anticounterfeiting, displays, sensors, and optical devices. What is more, it is effective not only for removing organic contaminants (such as VOCs) but also for reducing the industrial waste gas  $\text{CO}_2$  emissions which greatly protects the environment.

## Data Availability

(1) The HRTEM, AFM, PL spectra, Raman, FTIR, and fluorescent image data used to support the findings of this study are included within the article. (2) The additional HRTEM, UV-Vis spectra, Raman, FTIR, and GC-MS of other benzene series data used to support the findings of this study are included within the supplementary information file(s). (3) Previously reported data were used to support this study and are available at [doi:10.1039/c8ra03723j]. These prior studies (and datasets) are cited at relevant places within the text as references [20].

## Additional Points

*Notes and References.* In a typical procedure, styrene (0.208 g, Aladdin, purity  $>98\%$ ) and  $\text{H}_2\text{O}_2$  ( $400\ \mu\text{L}$ ) were added to  $\text{Cu}(\text{Ac})_2$  (0.4g) solution (10 mL) at  $60^\circ\text{C}$  under stirring for 12 h. The final CD-SAMFs were purified by extracting with butyl acetate and water several times to remove the impurities including the residual organic and inorganic molecules. Then, the purified CD-SAMFs were dried at  $60^\circ\text{C}$  for structural characterization and measurements. The synthetic procedure for the CDs by using other benzene series VOCs was similar to that of the styrene CDs except for the addition of different benzene series in the same media: 0.2 mol/L benzene, 0.2 mol/L benzyl alcohol, and 0.2 mol/L xylene.

## Conflicts of Interest

There are no conflicts to declare.

## Supplementary Materials

Figure S1: HRTEM of carbon dot self-assembled monolayer films (CD-SAMFs). (a, b) The related size distribution of carbon dots in the CD-SAMFs. Figure S2: UV-Vis spectra of the benzene series (a) and PL emission spectra of CDs by other benzene series: (b) benzene, (c) benzyl alcohol, and (d) xylene. Figure S3: Raman spectra of CDs synthesized by other benzene series. Figure S4: FTIR spectra of CDs synthesized by other benzene series. Table S1: GC-MS test. (*Supplementary Materials*)

## References

- [1] K. S. Novoselov, D. Jiang, F. Schedin et al., "Two-dimensional atomic crystals," *Proceedings of the National Academy of Sciences of the United States of America*, vol. 102, no. 30, pp. 10451–10453, 2005.
- [2] L. Hu, M. Chen, W. Shan et al., "Stacking-order-dependent optoelectronic properties of bilayer nanofilm photodetectors made from hollow ZnS and ZnO microspheres," *Advanced Materials*, vol. 24, no. 43, pp. 5872–5877, 2012.
- [3] H. Bao, C. M. Li, X. Cui, Q. Song, H. Yang, and J. Guo, "Single-crystalline Bi<sub>2</sub>S<sub>3</sub> nanowire network film and its optical switches," *Nanotechnology*, vol. 19, no. 33, article 335302, 2008.
- [4] A. A. Tahir, M. A. Ehsan, M. Mazhar, K. G. U. Wijayantha, M. Zeller, and A. D. Hunter, "Photoelectrochemical and photoresponsive properties of Bi<sub>2</sub>S<sub>3</sub> nanotube and nanoparticle thin films," *Chemistry of Materials*, vol. 22, no. 17, pp. 5084–5092, 2010.
- [5] S. Sahoo, S. Husale, B. Colwill, T. M. Lu, S. Nayak, and P. M. Ajayan, "Electric field directed self-assembly of cuprous oxide nanostructures for photon sensing," *ACS Nano*, vol. 3, no. 12, pp. 3935–3944, 2009.
- [6] W. Tian, C. Zhang, T. Zhai et al., "Flexible SnO<sub>2</sub> hollow nanosphere film based high-performance ultraviolet photodetector," *Chemical Communications*, vol. 49, no. 36, pp. 3739–3741, 2013.
- [7] W. Tian, T. Zhai, C. Zhang et al., "Low-cost fully transparent ultraviolet photodetectors based on electrospun ZnO-SnO<sub>2</sub> heterojunction nanofibers," *Advanced Materials*, vol. 25, no. 33, pp. 4625–4630, 2013.
- [8] H. Y. Kim, D.-E. Yoon, J. Jang et al., "Quantum dot/siloxane composite film exceptionally stable against oxidation under heat and moisture," *Journal of the American Chemical Society*, vol. 138, no. 50, pp. 16478–16485, 2016.
- [9] R. Liang, D. Yan, R. Tian et al., "Quantum dots-based flexible films and their application as the phosphor in white light-emitting diodes," *Chemistry of Materials*, vol. 26, no. 8, pp. 2595–2600, 2014.
- [10] X. Liu, X. Zhang, R. Wu et al., "All-quantum-dot emission tuning and multicolored optical films using layer-by-layer assembly method," *Chemical Engineering Journal*, vol. 324, pp. 19–25, 2017.
- [11] S. Y. Lim, W. Shen, and Z. Gao, "Carbon quantum dots and their applications," *Chemical Society Reviews*, vol. 44, no. 1, pp. 362–381, 2015.
- [12] S. N. Baker and G. A. Baker, "Luminescent carbon nanodots: emergent nanolights," *Angewandte Chemie International Edition*, vol. 49, no. 38, pp. 6726–6744, 2010.
- [13] L. Camilli, J. H. Jørgensen, J. Tersoff et al., "Self-assembly of ordered graphene nanodot arrays," *Nature Communications*, vol. 8, no. 1, p. 47, 2017.
- [14] B. Wang, Y. Chen, Y. Wu et al., "Aptamer induced assembly of fluorescent nitrogen-doped carbon dots on gold nanoparticles for sensitive detection of AFB<sub>1</sub>," *Biosensors and Bioelectronics*, vol. 78, pp. 23–30, 2016.
- [15] K. T. Narasimha, C. Ge, J. D. Fabbri et al., "Ultralow effective work function surfaces using diamondoid monolayers," *Nature Nanotechnology*, vol. 11, no. 3, pp. 267–272, 2016.
- [16] J. Mao, X. Y. Kong, D. Wang, and Z. Zou, "Assembly of metallic carbon nanodots aligned on a vicinal Si (111)-7×7 surface," *Journal of the American Chemical Society*, vol. 129, no. 13, pp. 3782–3783, 2007.
- [17] L. Schmidlin, V. Pichot, S. Josset et al., "Two-dimensional nanodiamond monolayers deposited by combined ultracentrifugation and electrophoresis techniques," *Applied Physics Letters*, vol. 101, no. 25, article 253111, 2012.
- [18] C. J. Tang, S. M. S. Pereira, A. J. S. Fernandes et al., "Synthesis and structural characterization of highly <100>-oriented {100}-faceted nanocrystalline diamond films by microwave plasma chemical vapor deposition," *Journal of Crystal Growth*, vol. 311, no. 8, pp. 2258–2264, 2009.
- [19] N. R. Greiner, D. S. Phillips, J. D. Johnson, and F. Volk, "Diamonds in detonation soot," *Nature*, vol. 333, no. 6172, pp. 440–442, 1988.
- [20] L. Bao, C. Liu, Z.-L. Zhang, and D.-W. Pang, *Advanced Materials*, vol. 27, no. 10, pp. 1663–1667, 2015.
- [21] Y.-P. Sun, B. Zhou, Y. Lin et al., "Quantum-sized carbon dots for bright and colorful photoluminescence," *Journal of the American Chemical Society*, vol. 128, no. 24, pp. 7756–7757, 2006.
- [22] S. C. Hess, F. A. Permatasari, H. Fukazawa et al., "Direct synthesis of carbon quantum dots in aqueous polymer solution: one-pot reaction and preparation of transparent UV-blocking films," *Journal of Materials Chemistry A*, vol. 5, no. 10, pp. 5187–5194, 2017.
- [23] W. Y. Fan, J. Röpcke, and P. B. Davies, "Effect of oxygen on methyl radical concentrations in a CH<sub>4</sub>/H<sub>2</sub> chemical vapor deposition reactor studied by infrared diode laser spectroscopy," *Journal of Vacuum Science & Technology A: Vacuum, Surfaces, and Films*, vol. 14, no. 5, pp. 2970–2972, 1996.
- [24] H. Guo, B. You, S. Zhao et al., "Full-color tunable photoluminescent carbon dots based on oil/water interfacial synthesis and their applications," *RSC Advances*, vol. 8, no. 42, pp. 24002–24012, 2018.
- [25] S. Zhu, Q. Meng, L. Wang et al., "Highly photoluminescent carbon dots for multicolor patterning, sensors, and bioimaging," *Angewandte Chemie*, vol. 125, no. 14, pp. 4045–4049, 2013.
- [26] S. Qu, X. Wang, Q. Lu, X. Liu, and L. Wang, "A biocompatible fluorescent ink based on water-soluble luminescent carbon nanodots," *Angewandte Chemie, International Edition*, vol. 51, no. 49, pp. 12215–12218, 2012.
- [27] C. Popov, A. Gushterov, L. Lingys, C. Sippel, and J. P. Reithmaier, "Structural and optical properties of ultrananocrystalline diamond/InGaAs/GaAs quantum dot structures," *Thin Solid Films*, vol. 518, no. 5, pp. 1489–1492, 2009.
- [28] G. Zhang, L. J. Guo, Z. Liu, and X. Zheng, "Application of diamond-like carbon film as protection and antireflection coatings of ZnS elements," *Optical Engineering*, vol. 33, no. 4, pp. 1330–1334, 1994.

